Published in final edited form as:
J Immunol. 2008 November 1; 181(9): 6644–6653.

Immunization with a Mimotope of GD2 Ganglioside Induces CD8+ T Cells That Recognize Cell Adhesion Molecules on Tumor Cells[1]

Andrzej Wierzbicki[2,3,*], **Margaret Gil**[2,*], **Michael Ciesielski**[†], **Robert A. Fenstermaker**[†], **Yutaro Kaneko**[‡], **Hanna Rokita**[§], **Joseph T. Lau**[¶], and **Danuta Kozbor**[4,*]

[*]Department of Immunology, Roswell Park Cancer Institute, Buffalo, NY 14263 [†]Department of Neurosurgery, Roswell Park Cancer Institute, Buffalo, NY 14263 [¶]Department of Molecular and Cellular Biology, Roswell Park Cancer Institute, Buffalo, NY 14263 [‡]Institute of Immunotherapy for Cancer, Kinki University, Osaka, Japan [§]Faculty of Biotechnology, Jagiellonian University, Krakow, Poland

Abstract

The GD2 ganglioside expressed on neuroectodermal tumor cells has been used as a target for passive and active immunotherapy in patients with malignant melanoma and neuroblastoma. We have reported that immunization of mice with a 47-LDA mimotope of GD2, isolated from a phage display peptide library with anti-GD2 mAb 14G2a, induces MHC class I-restricted $CD8^+$ T cell responses to syngeneic neuroblastoma tumor cells. The cytotoxic activity of the vaccine-induced CTLs was independent of GD2 expression, suggesting recognition of a novel tumor-associated Ag cross-reacting with 47-LDA. Glycan microarray and immunoblotting studies using 14G2a mAb demonstrated that this Ab is highly specific for the entire carbohydrate motif of GD2 but also cross-reacts with a 105 kDa glycoprotein expressed by $GD2^+$ and $GD2^-$ neuroblastoma and melanoma cells. Functional studies of tumor cells grown in three-dimensional collagen cultures with 14G2a mAb showed decreases in matrix metalloproteinase-2 activation, a process regulated by the 105 kDa-activated leukocyte cell adhesion molecule (ALCAM/CD166). A recombinant CD166 glycoprotein was shown to be recognized by 14G2a Ab and inhibition of CD166 expression by RNA interference ablated the cell sensitivity to lysis by 47-LDA-induced $CD8^+$ T cells in vitro and in vivo. The binding of 14G2a to CD166 was not disruptable by a variety of exo- and endo-glycosidases, implying recognition of a non-glycan epitope on CD166. These results suggest that the vaccine-induced CTLs recognize a 47-LDA cross-reactive epitope expressed by CD166, and reveal a novel mechanism of induction of potent tumor-specific cellular responses by mimotopes of tumor-associated carbohydrate Ags.

Aberrant glycosylation that is one of the most constant traits of the malignant phenotype (1) has led to studies directed toward the development of synthetic carbohydrate-based anticancer vaccines. Although these vaccines elicit primary Ab responses (2,3), it would also be

[1]This work was supported by the National Institutes of Health grants R21EB008071 (to D.K.) and R21NS054167 (to R.A.F.), and by funds to commemorate Dr. Goro Chihara's research activity.

4Address correspondence and reprint requests to Dr. Danuta Kozbor, Department of Immunology, Roswell Park Cancer Institute, Elm and Carlton Streets, Buffalo, NY 14263. E-mail address: danuta.kozbor@roswellpark.org.
[2]A.W. and M.G. contributed equally to this work.
[3]Current address: Department of Biochemistry and Molecular Biology, University of Medical Sciences, Poznan, Poland.

Disclosures
The authors have no financial conflict of interest.

advantageous if T cells directed to tumor-associated carbohydrate Ags could be generated during the immunization process (4–7). In an effort to define strategies to induce cell-mediated immunity to carbohydrate Ags expressed on tumor cells, we have been developing peptide mimics of GD2 ganglioside expressed on neuroectodermal tumor cells including neuroblastoma, melanoma, and glioma (8). We have shown that a 47-LDA peptide mimic of GD2 ganglioside expressed in plasmid DNA and delivered to mice in combination with IL-15 and IL-21 genes induced GD2 cross-reactive Ab responses that inhibited tumor growth of human MV3 melanoma cells in the SCID mouse xenograft model (8,9). Unexpectedly, this vaccine also activated potent $CD8^+$ T cell responses when delivered simultaneously or 1 day after challenge with $GD2^+$ syngeneic NXS2 neuroblastoma tumor cells (9). Adoptive immunotherapy with $CD8^+$ T cells isolated from 47-LDA-immunized and cured mice exhibited antitumor activity associated with regression of NXS2 tumor growth and tumor-free survival (9). The isolated $CD8^+$ T cells lyzed syngeneic $GD2^+$ and also $GD2^-$ (Neuro2a) neuroblastoma cells in a MHC class I-restricted manner (9), which indicated that the cellular ligand shared by both neuroblastoma tumor cells is distinct from GD2 ganglioside.

To clarify the possibility of therapeutic application of the 47-LDA mimetic vaccine-induced cellular responses for malignant tumors, we analyzed the antitumor activity and antigenic epitope recognized by 47-LDA vaccine-induced $CD8^+$ T cell responses in tumor-free mice. This study was necessary in view of the possibility that the generation of the neuroblastoma-specific CTLs in the NXS2-challenged and immunized mice could be affected by Ab-mediated targeting of tumor Ags which, in the presence of NK cells, would lead to a greater accumulation of Ab-coated antigenic tumor cell debris for efficient cross-priming by dendritic cells (DCs) [5] (10–12). Alternatively, the 47-LDA peptide mimic could activate CTLs that recognize an unknown O-linked glycopeptide presented by MHC class I Ags (4), or a cross-reactive peptide epitope expressed by $GD2^-$ Neuro2a neuroblastoma cells. The most intriguing finding in the process of identifying the target molecule for the 47-LDA vaccine-induced CTLs was the discovery that the GD2-specific mAb 14G2a, which was originally used for isolation of the peptide mimic 47-LDA, cross-reacted with a 105 kDa glycoprotein expressed by murine and human neuroblastoma and melanoma cells. In this study, we present evidence that a 47-LDA cross-reactive epitope expressed by CD166 cell adhesion molecules is targeted by the vaccine-induced CTLs. Stable silencing of CD166 expression in $GD2^-$ Neuro2a cells by CD166-specific short-hairpin RNA (shRNA) not only decreased reactivity of these cells with 14G2a mAb but also abolished recognition by 47-LDA vaccine-induced $CD8^+$ T cells. The latter effect was also associated with resistance of Neuro2a cells with down-regulated CD166 expression to 47-LDA vaccine-induced antitumor protection in syngeneic mice.

Materials and Methods

Animals and cell lines

Female A/J mice, 6–8 wk of age, were obtained from The Jackson Laboratory. The experimental procedures were performed in compliance with protocols approved by the Institutional Animal Care and Use Committee of the Roswell Park Cancer Institute. The murine Neuro2a neuroblastoma cell line ($H\text{-}2K^kD^d$), designated formally as C1300 neuroblastoma, was obtained from the American Type Culture Collection (ATCC). The cells do not express b or c series gangliosides (13), and are MHC class I syngeneic to A/J mice (14). The murine NXS2 neuroblastoma cell line (provided by Dr. R. A. Reisfeld, the Scripps Research Institute, Department of Immunology, La Jolla, CA) is a hybrid between C1300 neuroblastoma and $GD2^+$ murine dorsal root ganglioma cells (14). The human HTLA230 neuroblastoma cell line

[5]Abbreviations used in this paper: DC, dendritic cell; ACT, adoptive cell transfer; BM, bone marrow; RFU, relative fluorescence unit; MMP-2, matrix metalloproteinase-2; ALCAM, activated leukocyte cell adhesion molecule; FAK, focal adhesion kinase; shRNA, short-hairpin RNA; RNAi, RNA interference.

(15) was provided by Dr. E. Bogenmann (The Saban Research Institute, Childrens Hospital Los Angeles, Los Angeles, CA), and human MV3 melanoma cell line (16) was provided by Dr. G. van Muijen (University of Nijmegen, Nijmegen, the Netherlands). The hybridoma cell line secreting GD2-specific mAb 14G2a (17) was provided by Dr. R. A. Reisfeld and hybridoma cell line secreting human CD3-specific mAb (OKT3) was purchased from ATCC.

Antibodies

mAbs 14G2a and OKT3 were purified from culture supernatants by affinity chromatography on the HiTrap Protein G HP column (Amersham Biosciences). mAb against mouse CD166 glycoprotein that cross-reacts with human CD166 molecules (1172) was purchased from R&D Systems, and mAb against MHC class I H-2D^d Ag (34–2-12) was purchased from BD Pharmingen. FITC-conjugated F(ab′)$_2$ fragment of goat anti-mouse or rat Ig Ab was purchased from ICN Pharmaceuticals. HRP-conjugated goat anti-mouse or rat IgG Ab was purchased from Sigma-Aldrich.

Immunization and tumor challenge

The construction of 47-LDA expression vector was reported elsewhere (8). A/J mice (n = 5) were immunized i.m. with 100 μg of the 47-LDA construct or sham vector in combination with 20 μg of IL-15 and IL-21 expression plasmids (InvivoGen) three times, every 14 days. The IL-15-encoded plasmid was delivered at the time of the 47-LDA immunization, whereas IL-21 vector was injected 5 days later as described (9). The analyses of the 47-LDA vaccine-induced CTL responses and tumor challenge were conducted 2 wk after the last immunization. For tumor challenge, the immunized A/J mice (n = 5–10) were injected s.c. in the lateral flank with NXS2, Neuro2a, or Neuro2a-cl #1 cells (2×10^6 cells per injection). Tumor growth was monitored by measuring s.c. tumors three times a week with a microcaliper and determining tumor volume (width × length × width/2 = mm^3).

CTL assay

Splenocytes from the immunized A/J mice were cultured with 47-LDA-transfected DCs at the 20:1 ratio as described (9). Before stimulation, CD8$^+$ splenocytes were isolated by negative selection using T cell enrichment columns (Miltenyi Biotec) according to the manufacturer's protocol. The cytolytic activity of CTLs against NXS2 and Neuro2a cells was analyzed 5 days later by a standard 4-h ^{51}Cr-release assay. The percent of specific lysis was calculated as: ([cpm experimental release − cpm spontaneous release]/[cpm maximum release − cpm spontaneous release]) × 100. Maximum release was determined from supernatants of cells that were lysed by addition of 5% Triton X-100. Spontaneous release was determined from target cells incubated with medium only.

Depletion of CD4$^+$ and CD8$^+$ cells

The 47-LDA vaccine-immunized A/J mice were injected i.p. with 100 μg of anti-CD4 mAb (GK 1.5) or anti-CD8 mAb (53–6.72) on days 3 and 1 before and days 1, 8, 15, and 22 after the challenge as described (9). The Ab treatment was capable of depleting CD4$^+$ and CD8$^+$ in nonimmunized mice by ~90% as determined by flow cytometric analyses with anti-CD4 (H129.19) and anti-CD8 (53–6.7) mAbs (BD Pharmingen), respectively. Control groups were treated with 100 μg of rat IgG (ICN Biomedical).

Generation of 47-LDA-transfected bone marrow-derived DCs

DCs were generated in vitro from bone marrow precursors as previously described (18). In brief, bone marrow cells were harvested from the tibias and femurs of 6- to 8-wk-old female A/J mice and then cultured in complete medium supplemented with 10 ng/ml GM-CSF at 37° C for 7 days. The medium was replenished every 2–3 days. On day 7, most of the nonadherent

cells had acquired DC morphology and were CD11c high and CD80, CD86, and MHC class II low, as determined by flow cytometric analyses. The immature DCs were transfected with the 47-LDA plasmid or sham vector using Lipofectamine 2000 (Invitrogen) according to the manufacturer's protocol. The cells were incubated for an additional 24 h with 100 ng/ml LPS to up-regulate expression of MHC class II, CD80, and CD86 (18), and used for stimulation of T cells.

Adoptive transfer of CD8$^+$ T cells

A/J mice (n = 6–8 for all groups) were injected s.c. with 2×10^6 NXS2 neuroblastoma cells and treated 15 days later by i.v. injection with CD8$^+$-enriched splenocytes isolated from 47-LDA vaccine-immunized syngeneic mice. For the adoptive cell transfer (ACT), CD8$^+$ T cells were negatively selected using paramagnetic Microbeads conjugated to anti-mouse CD4 (L3T4) and anti-mouse CD45R (B220) mAbs (MACS; Miltenyi Biotec) according to the manufacturer's instructions. The resulting populations consisted of >85% CD8$^+$ and ~10% CD4$^+$ splenocytes. The isolated CD8$^+$ splenocytes (2×10^7) were incubated overnight with 47-LDA-transfected DCs (20:1 ratio) in 15% T cell stimulatory factor (T-STIM Culture Supplement, Collaborative Biomedical Products) as a source of exogenous IL-2, and injected to NXS2-bearing mice that were irradiated before the ACT. The expression vector encoding IL-15 was delivered at the time of ACT whereas IL-21 gene was injected 5 days later as described (9). Lymphopenia in NXS2 tumor-bearing mice was induced by nonmyeloablative (5 Gy) or myeloablative (9 Gy) total body irradiation 1 day before ACT and vaccination. Bone marrow (BM; 10^7 cells) transfer on the day of irradiation (9 Gy) was required to rescue the mice from lethality. Control mice bearing 15-day-old established s.c. NXS2 tumors were irradiated with 5 Gy or 9 Gy plus BM transplant and treated with IL-15 and IL-21 cytokine-expressing vectors. Survival was defined as the point at which mice were sacrificed due to extensive tumor growth. Kaplan-Meier survival plots were prepared, and significance was determined using logrank Mantel-Cox method.

Glycan microarray analysis of mAb 14G2a

The glycan microarray analysis of 14G2a mAb (5 μg/ml) binding to 285 glycans in replicates of six followed by Alexa-488-conjugated secondary Ab was performed by the Consortium of Functional Glycomics (Emory University School of Medicine; http://www.functionalglycomics.org/glycomics/HServlet?operation=view&sideMenu=no&psId=primscreen_PA_v21_732_01032007). The highest and lowest point from each set of six replicates has been removed, therefore, the presented relative fluorescence unit (RFU) value for each glycan is the average of four values.

Immunoblotting and immunoprecipitation

Cells were harvested with 0.02% EDTA, washed in PBS, and solubilized in a lysis buffer (10 mM Tris-HCl (pH 7.4), 0.5% Nonidet P-40, 0.5 M NaCl, 1 mM phenylmethylsulphonyl fluoride). Cell lysates or the recombinant CD166-Fc fusion protein (R&D Systems) were subjected to 10% SDS-PAGE, transferred onto polyvinylidene difluoride membranes and incubated with 14G2a, 1172, or OKT3 mAb (3 μg/ml). Bands were developed with HRP-conjugated secondary Ab followed by ECL plus Western blotting detection system (Amersham Biosciences). For immunoprecipitation, cell lysates were incubated with 14G2a mAb (3 μg/ml) followed by incubation with 20 μl of protein G-Sepharose (1/1) (Amersham Biosciences). After washing, the precipitates were subjected to immunoblotting as described above. In some experiments cell lysates were treated with enzymatic deglycosylation kit (GK80110 and GK80115, Pro Zyme) consisting of enzymes removing all N-linked, simple O-linked and complex Core 2 O-linked carbohydrates according to the manufacturer's protocol.

CD166 gene-specific RNA interference and flow cytometry analysis

Neuro2a cells were transduced with the sequence-verified shRNA lentiviral plasmid DNA for mouse CD166 gene or control vector containing a non-targeting shRNA that activates the RNA interference (RNAi) pathway but does not target any human and mouse gene (MISSION; Sigma-Aldrich) according to the manufacturer's protocol. The CD166 shRNA-transduced clones selected in puromycin were analyzed by intracellular staining with anti-CD166 mAb 1172 followed by flow cytometry on FACScan.

Three-dimensional collagen degradation assay

Type I collagen (BD Biosciences) was diluted to 1.5 mg/ml with serum-free medium containing 2% FITC-labeled collagen monomers (Molecular Probes), added to 24-well plates (300 μl), and allowed to gel at 37°C for 30 min before adding cells (10^6) as described (19). Cells were incubated for 72 h at 37°C before collection of culture supernatants and solid-phase collagen. In some experiments, 30 μg/ml of 14G2a mAb, OKT3 mAb, or proteinase inhibitor mixture (Sigma-Aldrich) was added to the lattice before polymerization as well as to the supernatant. Protease inhibitor mixture did not affect cell viability in collagen as assessed by trypan blue exclusion. To measure FITC release, solid-phase collagen containing cells was pelleted, and FITC released into the culture supernatant was analyzed by spectrofluorometry. The 100% values were obtained by complete collagenase digestion of cell-free collagen lattices. Background fluorescence was obtained by pelleting nondigested cell-free lattices.

Effect of 14G2a mAb on cell growth in vitro

Neuro2a, HTLA230, and MV3 cells (1×10^5 cells/well) were seeded in 24-well plates in serum-containing medium and treated with 14G2a or OKT3 mAb (30 μg/ml). The cells were counted using the trypan blue exclusion method after 72 h of incubation at 37°C.

Gelatin zymography

Gelatinase activities in culture supernatants were determined using SDS-PAGE zymography as described previously (20). SDS-polyacrylamide gels were prepared with 9% acrylamide and 0.1% gelatin, and samples were electrophoresed in nonreducing conditions. Following removal of SDS through a 1-h incubation in 50 mM Tris-Cl (pH 7.4) containing 2% Triton X-100, the gels were incubated for 18 h at 37°C in 50 mM Tris-Cl (pH 7.4), 1% Triton X-100, and 5 mM $CaCl_2$, and stained with 0.5% Coomasie Brillant Blue R-250. The activation of MMP-2 was quantified using Molecular Imager Gel Doc XR System and Program Quantity One 4.6 from Bio-Rad Laboratories.

Statistical analyses

The statistical significance of the difference between groups was performed using a two-tailed Student's *t* test assuming equal variance. The *p* values for the pairwise group comparisons for the average tumor growth were computed using the nonparametric Wilcoxon's rank-sum test. Kaplan-Meier survival plots were prepared and median survival times were determined for tumor-challenged groups of mice. Statistical differences in the survival across groups were assessed using the logrank Mantel-Cox method. Data were presented as arithmetic mean ± SD and analyzed using the JMP program (SAS Institute) on a Windows-based platform.

Results

Immunization with the 47-LDA vaccine elicits antitumor $CD8^+$ T cell responses in A/J mice

To characterize the mechanisms of the generation of NXS2 neuroblastoma-specific CTLs by the 47-LDA vaccine, we first investigated whether the antitumor CTL responses could be induced during prophylactic immunization of syngeneic mice. A/J mice ($n = 5$) were

immunized three times with the 47-LDA mimotope DNA vaccine or sham vector in combination with IL-15 and IL-21 expression vectors in a 2-wk period of interval as described (9). The effector function of $CD8^+$ T cells was analyzed in a standard ^{51}Cr-release assay against syngeneic $GD2^+$ NXS2 and $GD2^-$ Neuro2a neuroblastoma cells. Allogeneic $GD2^+$ EL4 lymphoma ($H\text{-}2^b$) cells were used as a negative control. Fig. 1*A* shows that both NXS2 and Neuro2a cells were efficiently killed by the vaccine-induced $CD8^+$ T cells, whereas EL4 cells were resistant to the CTL-mediated killing. The cytotoxic activities against NXS2 and Neuro2a tumor cells were approximately 3-fold higher over a broad range of the E:T ratios compared with those measured in control animals, confirming that the Ag recognized by the 47-LDA vaccine-induced CTLs is distinct from GD2 ganglioside.

The antitumor activity of 47-LDA-induced immune response was also demonstrated in challenge experiments with NXS2 neuroblastoma injected s.c. into A/J mice ($n = 5–10$) 2 wk after immunization with the 47-LDA vector delivered in the presence of IL-15 and IL-21 genes. Untreated mice or those immunized with a sham plasmid in combination with IL-15 and IL-21 genes served as controls. As shown in Fig. 1*B*, all control mice developed palpable tumors within 20 days after the challenge and had to be sacrificed by day 40. In contrast, none of the immunized mice exhibited tumor growth on day 20. Three of ten mice that were immunized with the 47-LDA vaccine developed progressive tumor by day 40, and had to be sacrificed by days 63, 69, and 72. The remaining seven mice in this group had tumor-free survival for >100 days, reflecting a significant antitumor influence of the 47-LDA vaccine-induced immune responses compared with the control groups of animals ($p < 0.0001$).

In vivo efficacy of 47-LDA vaccine-induced $CD8^+$ T cells

Depletion studies of the vaccine-induced $CD8^+$ and $CD4^+$ T cells by Ab treatment were performed to determine the protective antitumor efficacy of the CTL responses. Fig. 2*A* shows that depletion of $CD8^+$ T cells almost completely abolished the vaccine-induced protection. In 47-LDA-immunized mice that were treated with anti-CD8 mAb, the mean rate of NXS2 tumor growth was similar to that measured in the sham vector-treated animals, suggesting the presence of functional $CD8^+$ effector T cells in 47-LDA-immunized mice. On the other hand, depletion of $CD4^+$ T cells at the time of tumor inoculation had no substantial effect on the extent of tumor protection when compared with that measured in fully immune-competent mice which were immunized with the 47-LDA vaccine.

We next performed ACT experiments to investigate the therapeutic efficacy of the 47-LDA vaccine-induced $CD8^+$ T cells against established NXS2 tumor growth in A/J mice. For the adoptive transfer, Ag-experienced $CD8^+$ splenocytes isolated from 47-LDA-immunized mice were incubated overnight with 47-LDA-transfected DCs and injected i.v. to NXS2 tumor-bearing mice in conjunction with IL-15 expression vector, followed by IL-21 plasmid delivered 5 days later. To enhance in vivo expansion of the adoptively transferred $CD8^+$-enriched splenocytes (21,22), the tumor-bearing mice were sublethally (5 Gy) irradiated or received a myeloablative (9 Gy) dose of total body irradiation accompanied by transplantation of syngeneic BM from naive mice. Fig. 2*B* shows that lymphodepletion with a nonmyeloablative (5 Gy) regimen before adoptive transfer of the vaccine-induced $CD8^+$ T cells had a small therapeutic effect ($p = 0.185$). Consistent with previous findings that intense lymphodepletion lowers the levels of suppressive elements and reduces the numbers of endogenous host cells that consume homeostatic cytokines thereby leading to improved tumor treatment (22–24), adoptive transfer of the 47-LDA vaccine-induced $CD8^+$ T cells mediated tumor regression that was strikingly better after a myeloablative (9 Gy) preparative regimen (Fig. 2*C*; $p = 0.014$). The antitumor efficacy of the ACT seems specific because all control animals which were irradiated with 5 Gy or 9 Gy plus BM transplant and treated with IL-15 and IL-21 cytokine-

expressing vectors developed progressively growing tumors and had to be sacrificed by day 30.

Glycan microarray and reactivity of 14G2a mAb with a 105 kDa Ag expressed by GD2$^+$ and GD2$^-$ tumor cells

It has become evident that both CD4$^+$ and CD8$^+$ T cells can recognize glycopeptides carrying mono- and disaccharides in a MHC-restricted manner providing that the glycan group is attached to the peptide at suitable positions (25). These findings raised a possibility that the 47-LDA peptide could mimic a mono- or disaccharide of GD2 ganglioside displayed by glycosylated tumor rejection Ag in GD2$^-$ Neuro2a cells. However, the reactivity patterns of 14G2a mAb with 285 glycans corresponding to carbohydrate residues of GD2 ganglioside in a glycan microarray analysis revealed that 14G2a Ab is highly specific for the entire carbohydrate motif of GD2 ganglioside displayed by five carbohydrate Neu5Acα2–8Neu5Acα2–3(GalNAcβ1–4)Galβ1–4Glcβ residues. As shown in Fig. 3*A*, the average RFU for the Neu5Acα2–8Neu5Acα2–3(GalNAcβ1–4)Galβ1–4Glcβ molecule was 44,508 ± 1,651, whereas addition of one or two Neu5Ac reduced the RFU values to 1,151 ± 192 and 3,433 ± 522, respectively. Similarly, deletion of a single carbohydrate residue within the Neu5Acα2–8Neu5Acα2–3(GalNAcβ1–4)Galβ1–4Glcβ core reduced the average RFU values to <600. The high specificity of 14G2a mAb for the intact carbohydrate motif of GD2 ganglioside was also consistent with the ability of the 47-LDA peptide and GD2 ganglioside, but not individual carbohydrates of GD2, to inhibit the binding of 14G2a mAb to GD2$^+$ IMR-32 neuroblastoma cells (8). Altogether, results of these comprehensive analyses suggest that it is unlikely that 14G2a mAb recognizes other glycan structures.

In a search of the putative 47-LDA cross-reactive epitope whose expression by tumor cells would facilitate recognition by 47-LDA vaccine-induced CTLs, we performed immunoblotting analyses using 14G2a mAb and lysates from Neuro2a neuroblastoma cells. Because Neuro2a cells do not express GD2 ganglioside due to lack of GD3 synthase (26), but are efficiently killed by 47-LDA vaccine-induced CTLs, we hypothesized that these cells express a carbohydrate GD2-like motif that is recognized by 14G2a mAb. To address this possibility, cell lysates from Neuro2a were analyzed by Western blotting with 14G2a Ab in addition to the human CD3-specific mAb OKT3, which served as an isotype control. Lysates from the weakly GD2$^+$ human MV3 melanoma cells were also included in the analysis to determine whether the same Ag is expressed by other malignancies of neuroectodermal origin. As shown in Fig. 3*B*, 14G2a mAb recognized a 105 kDa band in the analyzed tumor cells irrespective of the expression of GD2 ganglioside. The recognition seems to be specific since the 105 kDa band was not detected with OKT3 mAb and other bands, including the one of 39 kDa molecular mass that was prominent in cell lysates of MV3 melanoma, were recognized by both Abs.

To better characterize the nature of the 14G2a mAb-reactive band, cells lysates from Neuro2a and MV3 cells were treated with enzymes that remove all N-linked, simple O-linked, and complex Core 2 O-linked carbohydrates [N-glycanase, PNGase F, sialidase A, O-glycanase, β (1–4) galactosidase, β-N-acetylglucosaminidase] followed by SDS-PAGE and immunoblotting with 14G2a mAb. Figure *3C* shows that deglycosylation of the cell lysates did not affect recognition by 14G2a mAb, except for the ~15 kDa faster migration of the deglycosylated bands compared with their 105 kDa control counterparts. These results indicate that 14G2a mAb recognizes a glycosylated protein with a molecular mass of 105 kDa expressed by human and mouse neuroblastoma and melanoma cells.

We next performed a series of functional studies to investigate the effect of 14G2a mAb on growth properties of Neuro2a, MV3, and another GD2$^+$ human HTLA230 neuroblastoma cells within three-dimensional collagen matrices. These experiments were prompted by previous analyses which showed that GD2 ganglioside is functionally involved in cell adhesion mediated

by the interaction between integrins and the extracellular matrix (27–29). Based on these findings, we hypothesized that interaction of 14G2a Ab with its putative ligand may alter growth properties of the tumor cells within three-dimensional collagen lattices. Using Neuro2a, HTLA230, and MV3 cells and type I collagen, which is the prevalent matrix encountered by invasive carcinomas (30,31), we analyzed tumor cell dissemination and proteolytic degradation of extracellular matrix barriers in the presence or absence of 14G2a mAb. Equal numbers of Neuro2a, HTLA230, and MV3 cells were cultured on three-dimensional collagen lattices containing FITC-labeled collagen for 72 h, and the structural breakdown of the matrix fibers by the cells was analyzed by measuring the degradation of FITC-labeled collagen fibers using a quantitative three-dimensional fluorometric FITC release assay (19). Fig. 4*A* shows that upon migration within collagen, all cells released FITC-labeled collagen content with the highest releases of 46 ± 3% measured in MV3 cultures and less than 30% released by Neuro2a and HTLA230 cells. Protease inhibitor cocktail inhibited >85% of the cell-mediated FITC release, suggesting the existence of protease-dependent tumor cell dissemination. The presence of 14G2a mAb in the culture reduced the cell-mediated FITC release by 54% in Neuro2a, 59% in HTLA230, and 37% in MV3 cultures compared with control cells grown in media, whereas the same concentration of OKT3 mAb reduced the FITC release by <10%. The observed inhibition of tumor cells mediated collagenolysis within three dimensional collagen lattices by 14G2a mAb suggests that the 47-LDA-cross-reactive ligand of 14G2a Ab expressed by neuroblastoma and melanoma cells is involved in a cellular process leading to collagen degradation.

14G2a Ab inhibits three dimensional collagen gel culture stimulation of pro-MMP-2 processing

Previous studies have shown that cell-to-matrix interactions that lead to clustering of integrin β1 and activation of gelatinase A/matrix metalloproteinase-2 (MMP-2) are influenced by cell-to-cell adhesion and controlled by the 105 kDa glycoprotein known as activated leukocyte cell adhesion molecule (ALCAM)/CD166 (32). Therefore, we next assessed the effect of 14G2a mAb on pro-MMP-2 processing using conditioned media from the three dimensional collagen cultures of Neuro2a, HTLA230, and MV3 cells. The cells were plated at a high density of 10^6 cells per gel in the presence of OKT3 (control), 14G2a mAb, or protease inhibitor mixture, and conditioned media collected after 72 h of incubation were analyzed by gelatin zymography. Fig. 4*B* shows that medium from the control cultures treated with OKT3 mAb exhibited reproducible conversion of pro-MMP-2 (72 kDa) to active (58 kDa) MMP-2. The human MV3 melanoma cells showed the strongest expression of pro-MMP-2 with a prominent band corresponding to the active MMP-2 in control cultures, whereas MMP-2 activation was less efficient in Neuro2a and HTLA230 cells. As expected, MMP-2 activation was barely detectable in cultures treated with the protease inhibitor mixture. Addition of 14G2a mAb at a concentration of 30 μg/ml reduced 2- to 3-fold expression of MMP-2 compared with levels detected in the control cultures, with the most prominent effect detected in MV3 cells (Fig. 4*B*).

To establish whether the inhibition of MMP-2 activation was due to Ab-mediated suppression of cell proliferation, we next examined the effect of 14G2a mAb on cell growth by adding 30 μg/ml of the Ab to the culture medium for 72 h. Fig. 4*C* shows that treatment of Neuro2a and HTLA230 cells with 14G2a mAb inhibited cell proliferation by 30 and 39% compared with the respective cultures treated with the same concentration of OKT3 mAb. Among the analyzed cultures, growth of MV3 cells exhibited the highest resistance to suppression by the 14G2a Ab treatment (Fig. 4*C*). Addition of 14G2a mAb inhibited proliferation of MV3 cells only by 14%, suggesting that the 3-fold reduction in MMP-2 expression by 14G2a mAb was caused by the interference of 14G2a mAb with MMP-2 activation in collagen cultures rather than reduced viability of the tumor cells.

Reactivity of 14G2a mAb with CD166 glycoprotein

Current models state that the assembly of a ternary complex of MT1-MMP, TIMP-2, and pro-MMP-2 involved in the MMP-2 activation cascade requires cell-to-cell adhesion, intact CD166 expression, and integrin clustering (32). The analyzed Neuro2a, MV3, and HTLA230 cells were found to express CD166 based on staining with CD166-specific 1172 mAb followed by flow cytometry analysis (data not shown). These results, together with the ability of 14G2a mAb to bind to the 105 kDa glycoprotein in Neuro2a, MV3, and HTLA230 cells and interfere with the CD166-mediated network of MMP-2 activation (32), suggested that 14G2a recognizes an antigenic epitope expressed by the CD166 glycoprotein. To address this hypothesis experimentally, we first investigated the binding of 14G2a mAb to the recombinant CD166 glycoprotein in the Western blotting analysis. CD166-specific 1172 mAb and OKT3 mAb were included in the assay as positive and negative controls, respectively. The recombinant CD166 glycoprotein used in the study was a glycosylated disulfide-linked homodimeric protein expressed as an extracellular domain of human CD166 (aa 1–526) fused to the carboxy-terminal 6x histidine-tagged Fc region of human IgG1 via a polypeptide linker (CD166-Fc). Fig. 4*D* shows that both 1172 and 14G2a mAbs recognized a 120 kDa band corresponding to the CD166-Fc fusion protein, whereas immunoblotting with OKT3 mAb was at a background level. The binding of 1172 Ab to CD166-Fc was approximately 3-fold higher than that of 14G2a reflecting either differences in reactivity of these Abs under denaturing conditions or a higher specificity of the former Ab for its cognate epitope on CD166.

Although the binding of 14G2a Ab to the recombinant CD166 fusion protein supported the molecular mimicry between an antigenic epitope expressed by CD166 and the 47-LDA mimotope of GD2 ganglioside, it did not rule out the possibility that other Ags expressed in the neuroblastoma and melanoma cells with a sequence similarity to CD166 may be recognized by 14G2a Ab. Therefore, we next investigated whether down-regulation of CD166 expression in Neuro2a cells by the RNA interference approach would ablate binding of 14G2a mAb. In the CD166 knockout experiments, Neuro2a cells were transduced with a lentivirus plasmid DNA-expressing shRNA for stable CD166 gene silencing. Cells transduced with a vector containing a nontargeting shRNA that activates the RNAi pathway but does not target any human and mouse gene (Neuro2a-control) were included as a control to determine whether the reduction in CD166 expression was specific for CD166. The transduced cells were selected in puromycin-containing medium and analyzed for CD166 expression by intracellular staining with 1172 mAb. In all CD166 shRNA-transduced Neuro2a clones, the reduction in CD166 expression levels ranged from 40 to 70% and correlated with lower 14G2a Ab staining (data not shown). Among the analyzed clones, Neuro2a-cl number 1 cells exhibited the lowest intracellular expression of CD166 compared with the parental Neuro2a and Neuro2a-control cells as determined by indirect immunofluorescence staining with 1172 mAb (Fig. 5*A*). A similar profile of staining was detected with 14G2a mAb (Fig. 5*B*). On the other hand, all analyzed cells exhibited comparable levels of H-2D^{d} Ag expression (Fig. 5*C*).

Effect of down-regulation of CD166 expression in Neuro2a cells on recognition by 47-LDA vaccine-induced cellular responses

We next examined the effect of reduced CD166 expression in Neuro2a cells on killing by 47-LDA vaccine-induced CD8^{+} T cells in vitro and in Neuro2a tumor-bearing mice. For the ^{51}Cr-release assay against Neuro2a-cl number 1 cells, CD8^{+} splenocytes were isolated from 47-LDA- or sham plasmid-immunized A/J mice. Parental Neuro2a cells or cells transduced with the control vector were also included in the assay. As shown in Fig. 6, *A* and *B*, Neuro2a cells were efficiently killed by the 47-LDA vaccine-induced CD8^{+} T cells, whereas these responses were at a background level with Neuro2a-cl number 1 cells used as targets. These results indicate that the down-regulation of CD166 expression rendered the tumor cells resistant to killing by 47-LDA-induced CTLs.

The significance of the evasion of Neuro2a cells with down-regulated CD166 from recognition by the 47-LDA vaccine-induced CTLs was also investigated during challenge studies by analyzing the ability of Neuro2a-cl number 1 cells to form tumor in 47-LDA-immunized mice. Groups of A/J mice ($n = 5$) were injected s.c. with 2×10^6 Neuro2a or Neuro2a-cl number 1 cells 2 wk after the third booster immunization with the 47-LDA vaccine delivered in combination with IL-15 and IL-21 genes. Tumor-challenged mice that were immunized with the sham plasmid instead of 47-LDA expression vector served as controls. As shown in Fig. 6, *C* and *D*, the control mice challenged with Neuro-2a and Neuro2a-cl number 1 cells exhibited progressive tumor growth and had to be sacrificed by days 20 and 26, respectively. Four out of five mice immunized with the 47-LDA vaccine and challenged with Neuro2a cells remained tumor-free and only one mouse developed palpable tumor within 2 wk after the challenge (Fig. 6*C*). In contrast, all 47-LDA-immunized mice that were challenged with Neuro2a-cl number 1 developed progressive tumors by day 15 after tumor inoculation and were sacrificed by day 26 (Fig. 6*D*). No significant decreases in the mean rate of Neuro2a-cl number 1 tumor growth were observed in the 47-LDA-immunized mice compared with the control animals, indicating that the down-regulation of CD166 expression conferred resistance to the 47-LDA vaccine-induced antitumor protection.

Discussion

Tumor-associated carbohydrate Ags are abundantly expressed on the surface of malignant cells and induction of cell-mediated immune responses toward them with peptide mimics may have outstanding applications in cancer immunotherapy. However, mechanisms underlying the phenomenon of molecular mimicry between the carbohydrate Ags and their mimotopes are poorly understood. In one report, it has been shown that a peptide surrogate of O-β-linked N-acetylglucosamine activates cross-reactive CTLs that recognize a processed O-linked glycopeptide associated with MHC class I molecules (4). Other investigators have demonstrated induction of carbohydrate-specific unrestricted CTL responses with MHC class I-binding carrier peptides (33). In our studies, however, anti-MHC class I Ab blocked CTL killing of the syngeneic NXS2 neuroblastoma cells (9), and an extensive lectin binding studies (4) together with the glycan profile of 14G2a mAb failed to demonstrate that the 47-LDA peptide simulates a carbohydrate residue of GD2 ganglioside which could be presented by O-β-linked glycopeptides in the context of MHC class I molecules to the 47-LDA vaccine-induced CTLs. On the contrary, the immunoprecipitation studies combined with down-regulation of CD166 expression by siRNA silencing suggested that the 47-LDA mimotope of GD2 ganglioside induces antitumor $CD8^+$ T cell responses to an antigenic epitope expressed by CD166 cell adhesion molecules. This novel finding highlights a new application of peptide mimotopes for immune therapy of cancer.

For many years, GD2 ganglioside has been considered to be a marker of neuroectoderm-derived human cancers without specific biological function in the malignant properties of human cancer cells. Colocalization of GD2 ganglioside at the adhesion plaques of melanoma cells and its functional involvement in a cell adhesion process mediated by the interaction between integrins and the extracellular matrix was first reported by Cheresh et al. (28). More recent studies revealed that GD2 ganglioside, integrin β1, and focal adhesion kinase (FAK) form a molecular complex across the plasma membrane, and Ab binding to GD2 induces conformational changes in integrin molecules leading to dephosphorylation of FAK and apoptosis associated with disruption of cell-matrix interaction, known as anoikis (34). Although results of this study elucidated, at least partly, the molecular association of GD2 with integrin and FAK molecules, it did not determine whether this interaction is direct or mediated by other membrane-penetrating molecules including cell adhesion molecules.

Cell adhesion molecules are involved in cell-cell and cell-matrix interactions, and are among the primary determinants of tissue architecture. ALCAM/CD166 is a member of the Ig superfamily, belonging to a subgroup with five extracellular Ig-like domains (VVC2C2C2), which includes MCAM/CD146/MUC18 and B-CAM/Lutheran (35,36). ALCAM/CD166 mediates cell-cell clustering through homophilic (ALCAM-ALCAM) and heterophilic (ALCAM-CD6) interactions, and while present in a wide variety of tissues, expression of CD166 is usually restricted to subsets of cells involved in dynamic growth and/or migration (reviewed in Ref. 36). Recent structure-function analyses have shown that homophilic CD166-mediated cell-cell adhesion is regulated through actin cytoskeleton-dependent clustering of CD166 molecules at the cell surface and that this clustering of CD166 is necessary to obtain stable adhesive interactions (37). In addition, CD166 regulates matrix metalloproteinase (MMP) activity and acts as a cell sensor for cell density, controlling the transition between local cell proliferation and tissue invasion in melanoma progression (37). In human melanoma cells, expression of CD166 glycoprotein and MMP-2 activation correlates strongly with metastatic potential and advanced melanoma tumor progression (38,39), and CD166 expression was observed at the tumor cell invasive front phase of vertical growth (39). Thus, the similarity between CD166 and GD2 ganglioside in their expression profile and involvement in cell adhesion process mediated by the interaction between integrins and the extracellular matrix suggests that both molecules could contribute to the metastatic process of tumor cell dissemination (40). The ability of 14G2a mAb to inhibit CD166-dependent MMP-2 activation in three dimensional collagen lattices may unravel complexity of this network. Furthermore, identification of the putative carbohydrate motif of GD2 within CD166, or perhaps other members of the cell adhesion molecules with a high sequence homology to CD166 (41), would be critical in understanding its functional significance in cell-cell and cell-matrix interactions, and may lead to discovery of therapeutic agents that disrupt adhesion or normalize signaling.

It is unlikely that CD166 expressed by Neuro2a cells carries the GD2 carbohydrate structure because Neuro2a lacks a critical enzyme for construction of GD2. However, the possibility remains that CD166 carries a peptide region that mimics GD2. Using the LALING program (www.ch.embnet.org) to find the best sequence alignment, we have identified only 13% identity between the entire 15-aa peptide 47-LDA and murine CD166 Ag. This finding precluded the possibility that the carbohydrate motif of GD2 ganglioside recognized by 14G2a mAb is expressed as a linear epitope within CD166. It rather argues that the 14G2a Ab recognizes a conformation-dependent epitope formed by stretches of amino acids located in various regions of the CD166 molecule. Consistent with this hypothesis, we identified a region ERTVNSLNVSA (aa 492–502) within CD166 with 36.4% identity in the 11 aa overlap with 47-LDA mimotope. The presence of Lys498 and Ala502 residues within this sequence stretch, which have been previously found as critical in the interaction between 47-LDA peptide and the 14G2a Ab-combining site (8), suggests that this region may be involved in the 14G2a mAb recognition. This possibility is also supported by the presence of H-2K^k binding motif ERTVNSLNV (aa 492–500) within the same sequence stretch of CD166. The latter sequence has 33.3% identity in the 9 aa overlap with 47-LDA peptide and an estimated score of 13, based on the SYFPEITHI epitope prediction algorithm (www.syfpeithi.de). Stimulation of splenocytes from 47-LDA vaccine-immunized A/J mice with ERTVNSLNV peptide revealed ~2-fold increases in the number of IFN-γ-secreting CD8$^+$ T cells compared with control cultures that were stimulated with an irrelevant peptide (data not shown). The CTL epitope mapping experiments of CD166 regions with increased similarities to the 47-LDA mimotope (42) are in progress to characterize CD8$^+$ T cell responses induced by the 47-LDA vaccine. Such analysis would also help to determine whether it is possible for the 47-LDA mimotope of GD2 to activate T cells specific for CD166 peptide, and whether a specific post-translational modification could affect the recognition. Consequently, this work would further extend our notion of vaccine design for cancer immunotherapy. Furthermore, the availability of antitumor

vaccines capable of inducing $CD8^+$ T cell responses to adhesion molecules may facilitate inhibition of metastatic tumor growth.

Acknowledgments

We are grateful to Drs. R. A. Reisfeld, E. Bogenmann and G. van Muijen for the reagents. We thank Dr. Joseph Missert for help in a quantitative three-dimensional fluorometric FITC release assay, and Earl Timm for help with a flow cytometric analysis. Glycan specificity of antibody 14G2a was performed by the Glycan Array Screening Core of the Consortium for Functional Glycomics.

References

1. Hakomori S. Aberrant glycosylation in tumors and tumor-associated carbohydrate antigens. Adv. Cancer Res 1989;52:257–331. [PubMed: 2662714]
2. Livingston PO, Ritter G, Calves MJ. Antibody response after immunization with the gangliosides GM1, GM2, GM3, GD2, and GD3 in the mouse. Cancer Immunol Immunother 1989;29:179–184. [PubMed: 2731184]
3. Livingston PO, Ragupathi G. Carbohydrate vaccines that induce antibodies against cancer: 2. Previous experience and future plans. Cancer Immunol. Immunother 1997;45:10–19. [PubMed: 9353422]
4. Monzavi-Karbassi B, Luo P, Jousheghany F, Torres-Quinones M, Cunto-Amesty G, Artaud C, Kieber-Emmons T. A mimic of tumor rejection antigen-associated carbohydrates mediates an antitumor cellular response. Cancer Res 2004;64:2162–2166. [PubMed: 15026358]
5. Jensen T, Hansen P, Galli-Stampino L, Mouritsen S, Frische K, Meinjohanns E, Meldal M, Werdelin O. Carbohydrate and peptide specificity of MHC class II-restricted T cell hybridomas raised against an O-glycosylated self peptide. J. Immunol 1997;158:3769–3778. [PubMed: 9103442]
6. Haurum JS, Arsequell G, Lellouch AC, Wong SY, Dwek RA, McMichael AJ, Elliott T. Recognition of carbohydrate by major histocompatibility complex class I-restricted, glycopeptide-specific cytotoxic T lymphocytes. J. Exp. Med 1994;180:739–744. [PubMed: 8046349]
7. Galli-Stampino L, Meinjohanns E, Frische K, Meldal M, Jensen T, Werdelin O, Mouritsen S. T-cell recognition of tumor-associated carbohydrates: the nature of the glycan moiety plays a decisive role in determining glycopeptide immunogenicity. Cancer Res 1997;57:3214–3222. [PubMed: 9242452]
8. Bolesta E, Kowalczyk A, Wierzbicki A, Rotkiewicz P, Bambach B, Tsao CY, Horwacik I, Kolinski A, Rokita H, Brecher M, et al. DNA vaccine expressing the mimotope of GD2 ganglioside induces protective GD2 cross-reactive antibody responses. Cancer Res 2005;65:3410–3418. [PubMed: 15833876]
9. Kowalczyk A, Wierzbicki A, Gil M, Bambach B, Kaneko Y, Rokita H, Repasky E, Fenstermaker R, Brecher M, Ciesielski M, Kozbor D. Induction of protective immune responses against NXS2 neuroblastoma challenge in mice by immunotherapy with GD2 mimotope vaccine and IL-15 and IL-21 gene delivery. Cancer Immunol Immunother 2007;56:1443–1458. [PubMed: 17597331]
10. Dhodapkar KM, Dhodapkar MV. Recruiting dendritic cells to improve antibody therapy of cancer. Proc. Natl. Acad. Sci. USA 2005;102:6243–6244. [PubMed: 15851655]
11. Groh V, Li YQ, Cioca D, Hunder NN, Wang W, Riddell SR, Yee C, Spies T. Efficient cross-priming of tumor antigen-specific T cells by dendritic cells sensitized with diverse anti-MICA opsonized tumor cells. Proc. Natl. Acad. Sci. USA 2005;102:6461–6466. [PubMed: 15824323]
12. Munz C, Steinman RM, Fujii S. Dendritic cell maturation by innate lymphocytes: coordinated stimulation of innate and adaptive immunity. J. Exp. Med 2005;202:203–207. [PubMed: 16027234]
13. Sato C, Matsuda T, Kitajima K. Neuronal differentiation-dependent expression of the disialic acid epitope on CD166 and its involvement in neurite formation in Neuro2A cells. J. Biol. Chem 2002;277:45299–45305. [PubMed: 12235144]
14. Lode HN, Xiang R, Dreier T, Varki NM, Gillies SD, Reisfeld RA. Natural killer cell-mediated eradication of neuroblastoma metastases to bone marrow by targeted interleukin-2 therapy. Blood 1998;91:1706–1715. [PubMed: 9473237]
15. Bogenmann E. A metastatic neuroblastoma model in SCID mice. Int. J. Cancer 1996;67:379–385. [PubMed: 8707412]

16. van Muijen GN, Jansen KF, Cornelissen IM, Smeets DF, Beck JL, Ruiter DJ. Establishment and characterization of a human melanoma cell line (MV3) which is highly metastatic in nude mice. Int. J. Cancer 1991;48:85–91. [PubMed: 2019461]

17. Mujoo K, Kipps TJ, Yang HM, Cheresh DA, Wargalla U, Sander DJ, Reisfeld RA. Functional properties and effect on growth suppression of human neuroblastoma tumors by isotype switch variants of monoclonal anti-ganglioside GD2 antibody 14.18. Cancer Res 1989;49:2857–2861. [PubMed: 2720646]

18. Brinker KG, Garner H, Wright JR. Surfactant protein A modulates the differentiation of murine bone marrow-derived dendritic cells. Am. J. Physiol 2003;284:L232–L241.

19. Wolf K, Mazo I, Leung H, Engelke K, von Andrian UH, Deryugina EI, Strongin AY, Brocker EB, Friedl P. Compensation mechanism in tumor cell migration: mesenchymal-amoeboid transition after blocking of pericellular proteolysis. J. Cell Biol 2003;160:267–277. [PubMed: 12527751]

20. Moser TL, Young TN, Rodriguez GC, Pizzo SV, Bast RC Jr, Stack MS. Secretion of extracellular matrix-degrading proteinases is increased in epithelial ovarian carcinoma. Int. J. Cancer 1994;56:552–559. [PubMed: 8112891]

21. Dudley ME, Wunderlich JR, Robbins PF, Yang JC, Hwu P, Schwartzentruber DJ, Topalian SL, Sherry R, Restifo NP, Hubicki AM, et al. Cancer regression and autoimmunity in patients after clonal repopulation with antitumor lymphocytes. Science 2002;298:850–854. [PubMed: 12242449]

22. Wrzesinski C, Paulos CM, Gattinoni L, Palmer DC, Kaiser A, Yu Z, Rosenberg SA, Restifo NP. Hematopoietic stem cells promote the expansion and function of adoptively transferred antitumor CD8 T cells. J. Clin. Invest 2007;117:492–501. [PubMed: 17273561]

23. Gattinoni L, Finkelstein SE, Klebanoff CA, Antony PA, Palmer DC, Spiess PJ, Hwang LN, Yu Z, Wrzesinski C, Heimann DM, et al. Removal of homeostatic cytokine sinks by lymphodepletion enhances the efficacy of adoptively transferred tumor-specific $CD8^+$ T cells. J. Exp. Med 2005;202:907–912. [PubMed: 16203864]

24. Gattinoni L, Powell DJ Jr, Rosenberg SA, Restifo NP. Adoptive immunotherapy for cancer: building on success. Nat. Rev. Immunol 2006;6:383–393. [PubMed: 16622476]

25. Werdelin O, Meldal M, Jensen T. Processing of glycans on glycoprotein and glycopeptide antigens in antigen-presenting cells. Proc. Natl. Acad. Sci. USA 2002;99:9611–9613. [PubMed: 12122209]

26. Kojima N, Kurosawa N, Nishi T, Hanai N, Tsuji S. Induction of cholinergic differentiation with neurite sprouting by de novo biosynthesis and expression of GD3 and b-series gangliosides in Neuro2a cells. J. Biol. Chem 1994;269:30451–30456. [PubMed: 7982960]

27. Cheresh DA, Harper JR. Arg-Gly-Asp recognition by a cell adhesion receptor requires its 130-kDa α subunit. J. Biol. Chem 1987;262:1434–1437. [PubMed: 2433281]

28. Cheresh DA, Harper JR, Schulz G, Reisfeld RA. Localization of the gangliosides GD2 and GD3 in adhesion plaques and on the surface of human melanoma cells. Proc. Natl. Acad. Sci. USA 1984;81:5767–5771. [PubMed: 6385004]

29. Cheresh DA, Pytela R, Pierschbacher MD, Klier FG, Ruoslahti E, Reisfeld RA. An Arg-Gly-Asp-directed receptor on the surface of human melanoma cells exists in an divalent cation-dependent functional complex with the disialoganglioside GD2. J. Cell Biol 1987;105:1163–1173. [PubMed: 2443507]

30. Azzam HS, Thompson EW. Collagen-induced activation of the M(r) 72,000 type IV collagenase in normal and malignant human fibroblastoid cells. Cancer Res 1992;52:4540–4544. [PubMed: 1322793]

31. Tomasek JJ, Halliday NL, Updike DL, Ahern-Moore JS, Vu TK, Liu RW, Howard EW. Gelatinase A activation is regulated by the organization of the polymerized actin cytoskeleton. J. Biol. Chem 1997;272:7482–7487. [PubMed: 9054450]

32. Lunter PC, van Kilsdonk JW, van Beek H, Cornelissen IM, Bergers M, Willems PH, van Muijen GN, Swart GW. Activated leukocyte cell adhesion molecule (ALCAM/CD166/MEMD), a novel actor in invasive growth, controls matrix metalloproteinase activity. Cancer Res 2005;65:8801–8808. [PubMed: 16204050]

33. Abdel-Motal UM, Berg L, Rosen A, Bengtsson M, Thorpe CJ, Kihlberg J, Dahmen J, Magnusson G, Karlsson KA, Jondal M. Immunization with glycosylated Kb-binding peptides generates

carbohydrate-specific, unrestricted cytotoxic T cells. Eur. J. Immunol 1996;26:544–551. [PubMed: 8605919]

34. Aixinjueluo W, Furukawa K, Zhang Q, Hamamura K, Tokuda N, Yoshida S, Ueda R, Furukawa K. Mechanisms for the apoptosis of small cell lung cancer cells induced by anti-GD2 monoclonal antibodies: roles of anoikis. J. Biol. Chem 2005;280:29828–29836. [PubMed: 15923178]
35. van Kempen LC, Nelissen JM, Degen WG, Torensma R, Weidle UH, Bloemers HP, Figdor CG, Swart GW. Molecular basis for the homophilic activated leukocyte cell adhesion molecule (ALCAM)-ALCAM interaction. J. Biol. Chem 2001;276:25783–25790. [PubMed: 11306570]
36. Swart GW. Activated leukocyte cell adhesion molecule (CD166/AL-CAM): developmental and mechanistic aspects of cell clustering and cell migration. Eur. J. Cell Biol 2002;81:313–321. [PubMed: 12113472]
37. Nelissen JM, Peters IM, de Grooth BG, van Kooyk Y, Figdor CG. Dynamic regulation of activated leukocyte cell adhesion molecule-mediated homotypic cell adhesion through the actin cytoskeleton. Mol. Biol. Cell 2000;11:2057–2068. [PubMed: 10848629]
38. Hofmann UB, Westphal JR, Waas ET, Zendman AJ, Cornelissen IM, Ruiter DJ, van Muijen GN. Matrix metalloproteinases in human melanoma cell lines and xenografts: increased expression of activated matrix metalloproteinase-2 (MMP-2) correlates with melanoma progression. Br. J. Cancer 1999;81:774–782. [PubMed: 10555745]
39. van Kempen LC, van den Oord JJ, van Muijen GN, Weidle UH, Bloemers HP, Swart GW. Activated leukocyte cell adhesion molecule/CD166, a marker of tumor progression in primary malignant melanoma of the skin. Am. J. Pathol 2000;156:769–774. [PubMed: 10702391]
40. Hakomori S. Cancer-associated glycosphingolipid antigens: their structure, organization, and function. Acta Anat 1998;161:79–90. [PubMed: 9780352]
41. Pires FR, Shih Ie M, da Cruz Perez DE, de Almeida OP, Kowalski LP. Mel-CAM (CD146) expression in parotid mucoepidermoid carcinoma. Oral Oncol 2003;39:277–281. [PubMed: 12618200]
42. Rock MT, Crowe JE Jr. Identification of a novel human leucocyte antigen-A*01-restricted cytotoxic T-lymphocyte epitope in the respiratory syncytial virus fusion protein. Immunology 2003;108:474–480. [PubMed: 12667209]

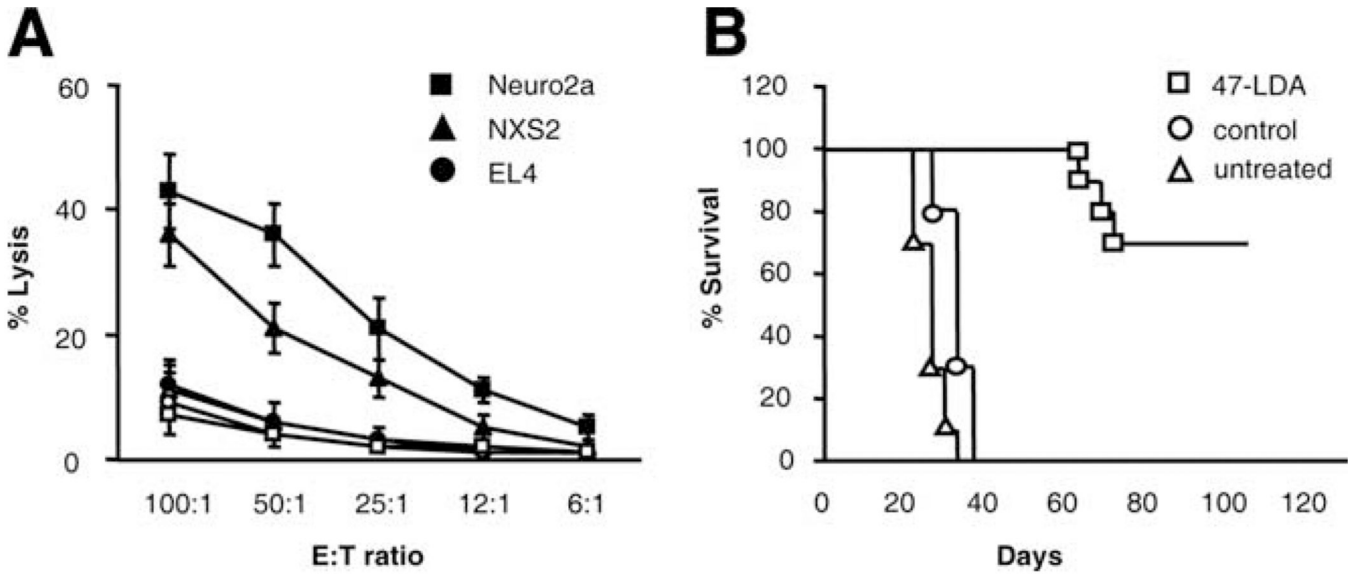

FIGURE 1.

Analyses of tumor-reactive $CD8^+$ T cell responses. *A*, CTL activities against NXS2 and Neuro2a neuroblastoma cells as well as EL4 lymphoma ($GD2^+$, $H\text{-}2^b$) cells in A/J mice immunized with the 47-LDA (closed symbols) or sham (open symbols) vector in the presence of IL-15 and IL-21 genes were analyzed in a standard ^{51}Cr-release assay. All determinants were made in triplicate samples, and the SD was <10%. Results are presented as the means ± SD of three independent experiments. *B*, Protective efficacy of the vaccine-induced immune responses against s.c. growth of NXS2 cells in A/J mice. Groups of five to ten mice that were immunized three times with the 47-LDA vaccine were challenged s.c. with 2×10^6 NXS2 cells as described in the Materials and Methods section. Untreated animals or those treated with the sham plasmid in combination with IL-15 and IL-21 served as negative controls. Survival was defined as the point at which mice were sacrificed due to extensive tumor growth. Kaplan-Meier survival plots were prepared and significance was determined using logrank Mantel-Cox method.

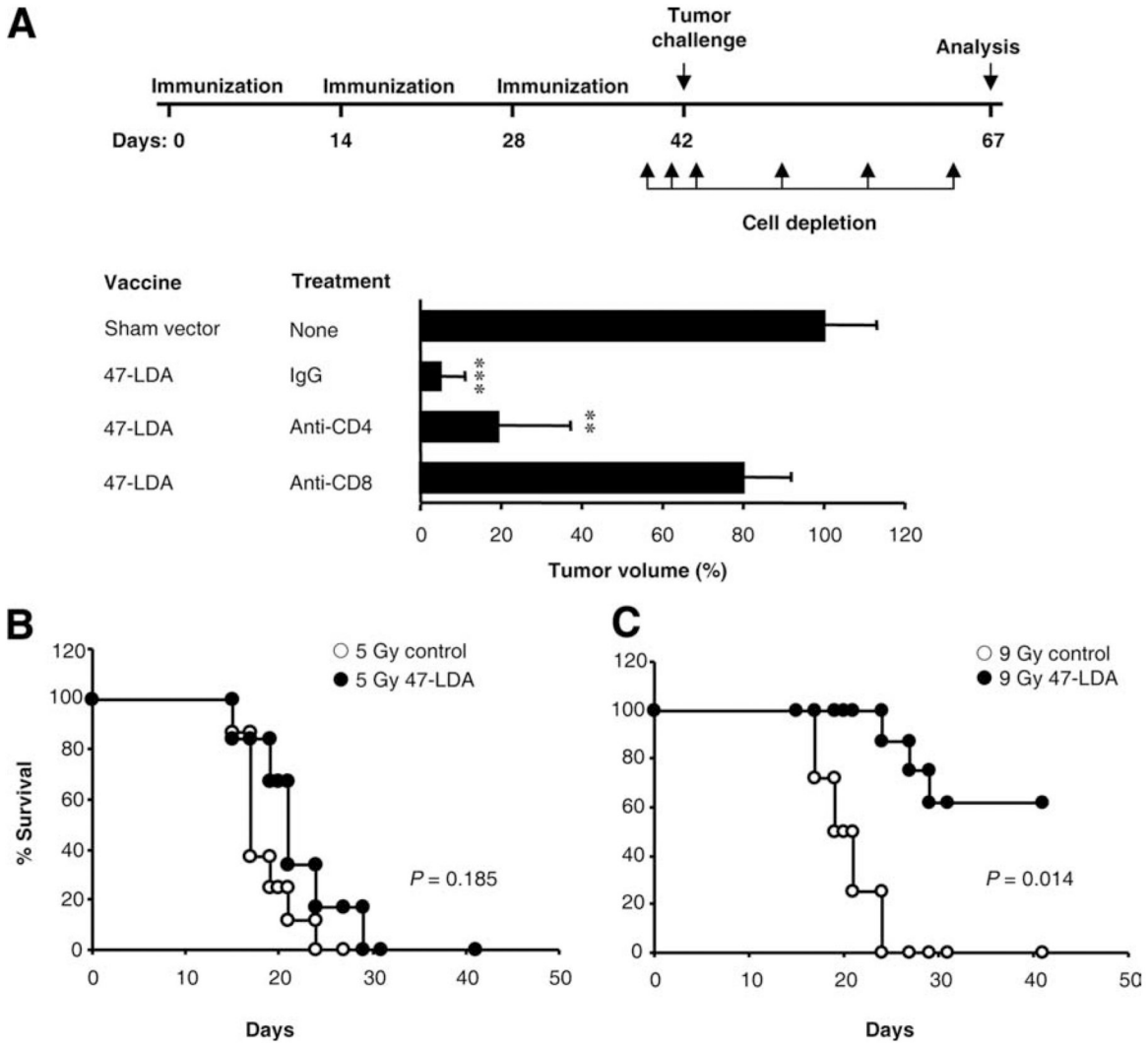

FIGURE 2.

Antitumor activity of 47-LDA vaccine-induced $CD8^+$ T cells in vivo. *A*, Protection against NXS2 tumor challenge requires 47-LDA vaccine-induced $CD8^+$ T cells. *Upper panel*, Schematic representation of the immunization schedule and depletion regimen. Lower panel depicts the effect of $CD4^+$ and $CD8^+$ cell depletion on tumor growth in the immunized and control A/J mice. The mean tumor growth in the control mice was measured 25 days after tumor inoculation and was considered as 100%. Bars, mean of experiments including five mice per group ± SD (error bars). **, $p < 0.001$; ***, $p < 0.0001$. *B*, Antitumor activities of adoptively transferred $CD8^+$ T cells from 47-LDA vaccinated mice. A/J mice ($n = 6–8$ for all groups) were injected s.c. with 2×10^6 Neuro2a neuroblastoma cells and treated 15 days later with i.v. adoptive transfer of $CD8^+$-enriched splenocytes isolated from 47-LDA-vaccinated syngeneic mice. Lymphopenia was induced by nonmyeloablative (5 Gy) or myeloablative (9 Gy) total body irradiation of tumor-bearing mice on the day of bone marrow (BM; 10^7 cells) transfer, which was 1 day before $CD8^+$ T cell transfer and vaccination. IL-15 and IL-21 genes were delivered at the time of immunization and 5 days later, respectively. NXS2 tumor-bearing mice that were irradiated with 5 Gy or 9 Gy plus BM transplant and treated with IL-15 and IL-21 cytokine-expressing vectors served as controls. Survival was defined as the point at which mice were sacrificed due to extensive tumor growth. Kaplan-Meier survival plots were prepared, and significance was determined using logrank Mantel-Cox method.

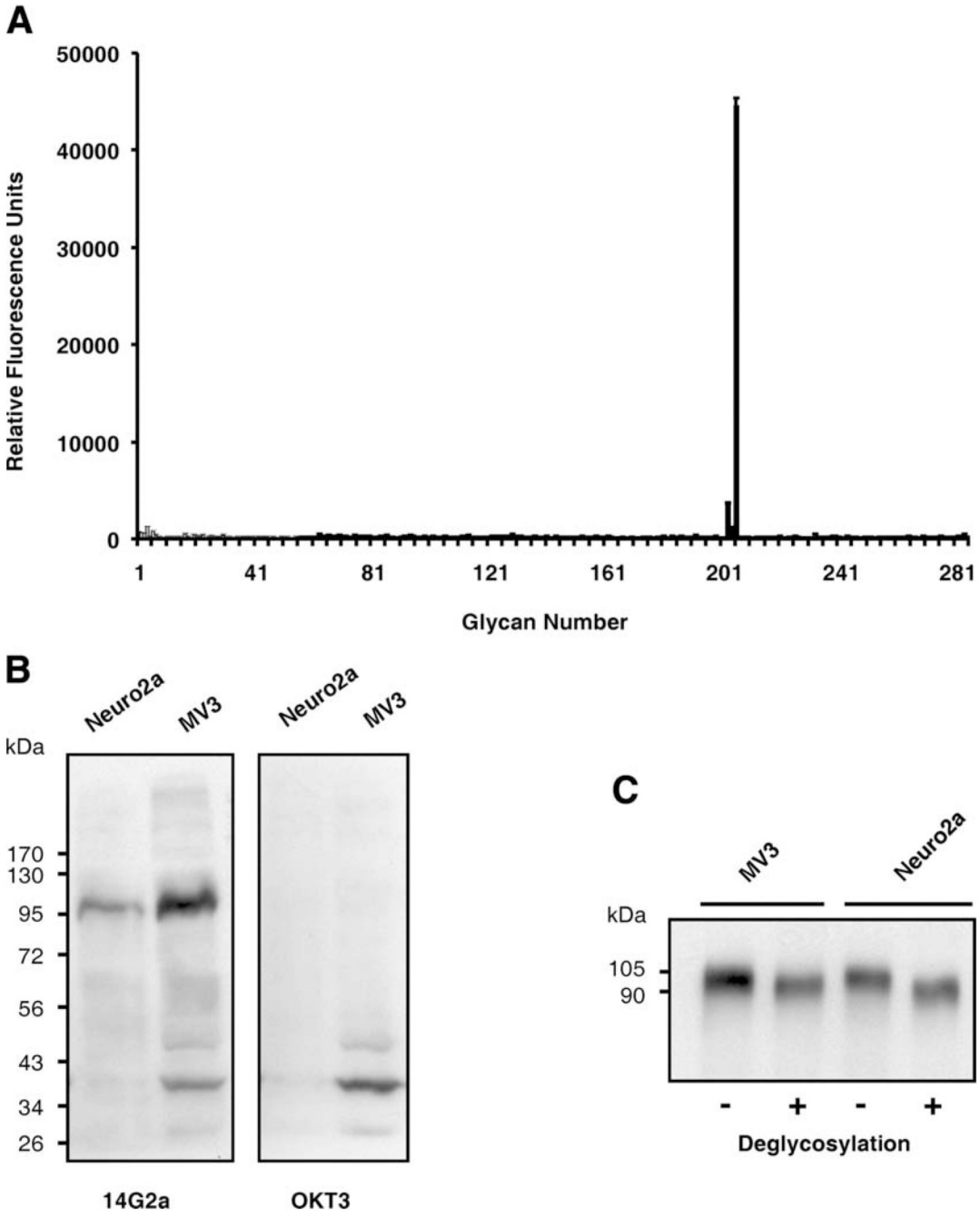

FIGURE 3.

Glycan microarray and immunoblotting with 14G2a mAb. *A*, The results of the glycan microarray analysis of 14G2a mAb, performed using 285 glycans in replicates of six followed by Alexa-488-conjugated secondary Ab, is publicly available at http://www.functionalglycomics.org/glycomics/HServlet?operation=view&sideMenu=no&psId=primscreen_PA_v21_732_01032007. The results are presented as the average RFU assay of four values ± SD. *B*, Immunoblotting of cell lysates from Neuro2a neuroblastoma and MV3 melanoma cells with 14G2a and OKT3 mAbs. The molecular masses of the standard proteins are shown on the left of the panels. *C*, Immunoblotting of deglycosylated Neuro2a and MV3 cell lysates with 14G2a mAb. The cell

lysates were deglycosylated using enzymatic deglycosylation kit before SDS-PAGE and immunoblotting with 14G2a mAb. Untreated cell lysates were included as controls.

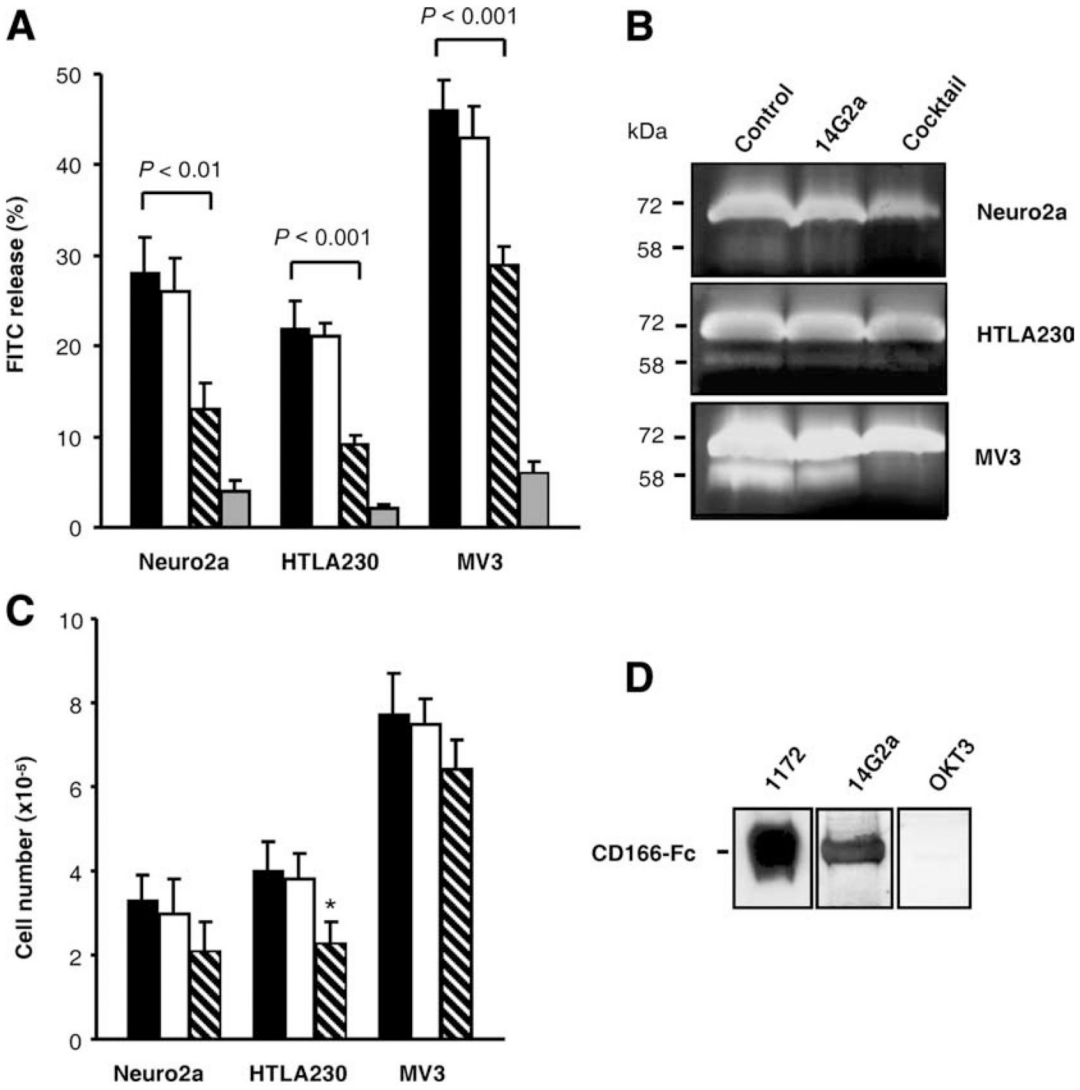

FIGURE 4.

Interaction of 14G2a mAb with recombinant and cellular CD166 glycoprotein. *A*, 14G2a mAb inhibits collagenolysis. Migration-associated collagenolysis caused by Neuro2a, HTLA230, and MV3 cells within three-dimensional FITC-collagen lattices was quantified from the FITC release after 72 h of migration in the presence or absence of inhibitors. Black, white, hatched, and gray bars denote cells cultured with medium, OKT3 mAb, 14G2a mAb, and the protease inhibitor cocktail. *B*, Inhibition of MMP-2 activation by 14G2a mAb. Neuro2a, HTLA230, and MV3 cell lines were cultured in collagen gels for 72 h. Conditioned media were analyzed by gelatin zymography to determine the level of MMP-2 activation. Position of 72 kDa pro-MMP-2 and 58 kDa active MMP-2 is indicated. *C*, Effect of 14G2a mAb on cell growth. Neuro2a, HTLA230, and MV3 cells were treated with 14G2a mAb (30 μg/ml) for 72 h and then counted with the trypan blue exclusion method. All determinants were made in triplicate samples, and the results are presented as the means ± SD of two independent experiments. *, $p < 0.05$. *D*, Western blotting analyses of recombinant CD166-Fc fusion protein (2 μg/lane) with mAbs specific for CD166 (1172), GD2 (14G2a), and CD3 (OKT3).

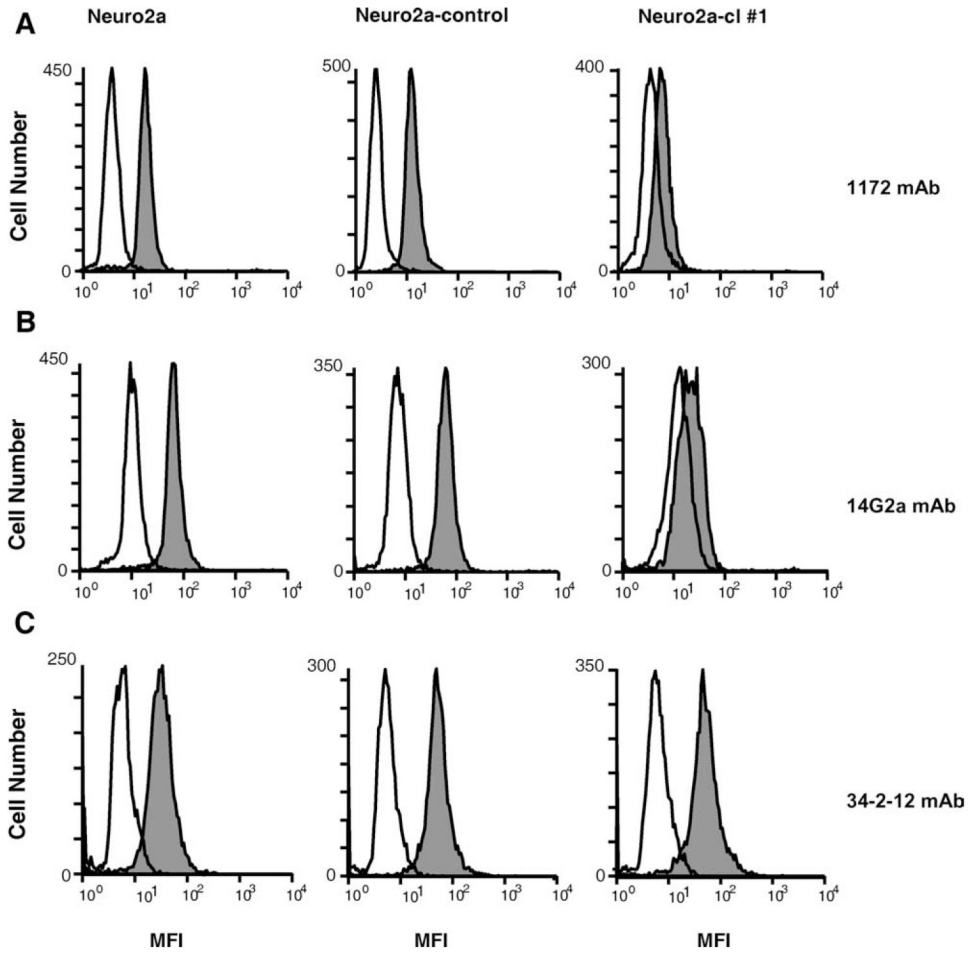

FIGURE 5.

Flow cytometry analyses of CD166 expression in CD166 shRNA-transduced Neuro2a-cl number 1 cells. Cells were stained intracellularly with anti-CD166 mAb 1172 (*A*), anti-GD2 mAb 14G2a (*B*), and anti-H-2D^d mAb 34–2-12 (*C*) followed by FITC-conjugated F(ab′)$_2$ portion of goat anti-mouse Ig. Cells were analyzed by flow cytometry on FACScan. Open histograms correspond to the isotype controls, and filled histograms show staining by the indicated mAbs.

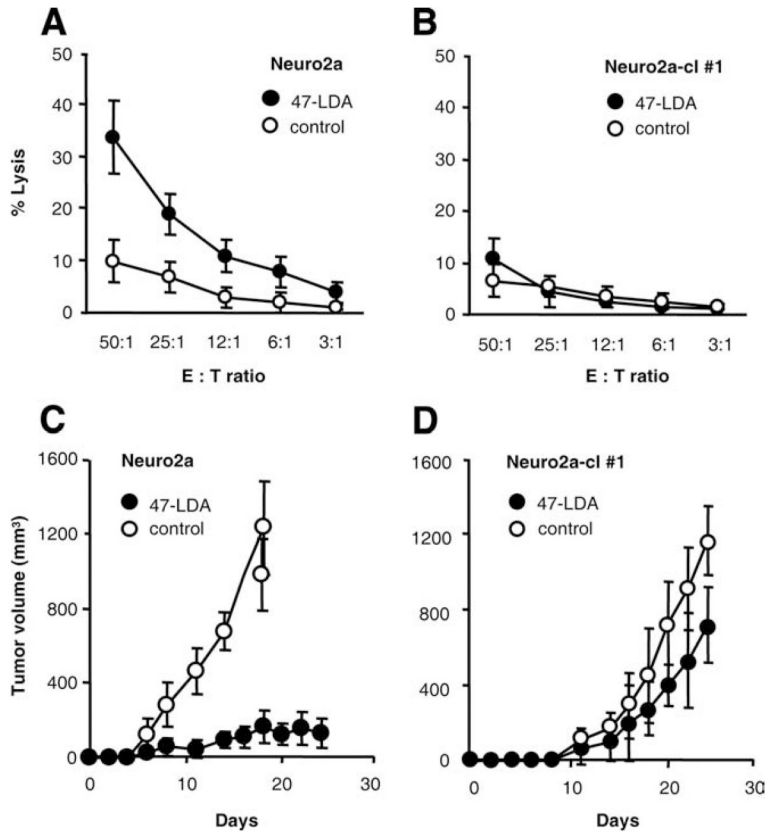

FIGURE 6.

Effect of down-regulation of CD166 expression on recognition by 47-LDA-induced cellular responses in vitro (*A* and *B*) and in vivo (*C* and *D*). CTL activities of 47-LDA vaccine-induced $CD8^+$ splenocytes in A/J mice against Neuro2a (*A*) and Neuro2a-cl number 1 (*B*) cells were analyzed in a standard ^{51}Cr-release assay. $CD8^+$ T cells from the sham plasmid-immunized mice were used as controls. All determinations were made in triplicate samples, and the SD was <10%. Results are presented as the means ± SD of three independent experiments. The effect of a prophylactic 47-LDA vaccine on Neuro2a (*C*) and Neuro2a-cl number 1 (*D*) tumor growth in A/J mice. Groups of A/J mice ($n = 5$) were immunized i.m. with the 47-LDA vaccine delivered in combination with IL-15 and IL-21 genes and injected s.c. with Neuro2a or Neuro2a-cl number 1 tumor (2×10^6 cells per injection) 2 wk after the third booster immunization. Tumor-challenged mice that were immunized with the sham plasmid served as controls. Animals were examined daily until the tumor became palpable, after which tumor growth was monitored by measuring s.c. tumors once to three times a week.